PHYSICAL REVIEW B **73**, 235308 (2006)

Structural stability and electronic structures of InP nanowires: Role of surface dangling bonds on nanowire facets

Toru Akiyama,* Kohji Nakamura, and Tomonori Ito
Department of Physics Engineering, Mie University, 1577 Kurima-Machiya, Tsu 514-8507, Japan

(Received 5 April 2006; published 6 June 2006)

The structural stability and electronic properties of InP nanowires (NWs) are investigated based on first-principles pseudopotential calculations. In contrast to the bulk phase, zinc-blende (ZB) NWs are found to be less favorable over wurtzite (WZ) NWs, in which the surface dangling bonds (DBs) on the NW facets play a crucial role to stabilize the WZ structure. Our analysis of the NW cohesive energy based on the number of DBs also suggests the bistability forming both ZB and WZ NWs around 120 Å diameter and the formation of rotational twin structures around 400 Å diameter being consistent with experiments. Furthermore, the stable WZ NWs are found to be semiconducting whose characteristics are dependent on the surface DBs as well as the NW size and shape. The estimated oscillator strength also indicates the possibility of efficient light emission originating from the direct gap and geometrically restricted excitonic effects.

DOI: 10.1103/PhysRevB.73.235308 PACS number(s): 81.07.Bc, 68.70.+w, 71.15.Nc, 73.20.At

I. INTRODUCTION

Semiconductor nanowires (NWs) grown by a vapor-liquid-solid mechanism[1] have great potential for understanding the fundamental roles of reduced dimensionality and size in optical, electrical, and mechanical properties and have been attracting great interest for their applications including photonics, nano and molecular electronics, and thermoelectrics.[2] So far, NWs of group-IV, -III-V, and -II-VI materials have been synthesized by employing various methods such as laser-assisted catalytic growth,[3–8] chemical vapor deposition,[9–14] metalorganic vapor-phase epitaxy,[15–19] and the other methods.[20–23] Moreover, for promising nanodevices based on the NWs, NWs with small diameters (~38 Å) are now designed by controlling the particle size of Au used as a catalyst for NW growth, as demonstrated in Si NWs.[14,23]

InP NWs in group-III-V NWs are one of the intriguing targets in the sources and detectors in fiber optic communications and high-speed electronic applications, such as *p-n* junction light-emitting diodes[5] and one-dimensional polarization-sensitive photodetectors.[7] In spite of this technological importance understanding of atomic structures and electronic properties of InP NWs still remains unclear. Recent observations by transmission electron microscopy (TEM) for an InP NW with a diameter of ~400 Å,[18] grown on InP(111) substrates, have suggested that the NWs seems to be zinc-blende (ZB) structures as seen in the bulk phase but they often contain rotational twin blocks, which are rotated by 60° with respect to each other. Since their rotational axis is the [111] direction, these twin blocks results in wurtzite- (WZ-) structured segments, implying that the relative stability between ZB and WZ structures in InP NWs is different from that of the bulk case. Furthermore, photoluminescence (PL) experiments[6,18] have observed a clear blueshift of the peak energy in NWs, suggesting a quantum confinement of the carriers.

Aside from these experimental investigations, little is so far known theoretically about the stable structures and electronic properties of group-III-V nanowires including InP NWs, although theoretical studies of Si NWs have been extensively carried out.[24–29] In particular, theoretical investigations concerning the stacking sequences of atomic layers along the growth direction have rarely been carried out. Therefore, precise predictions for the structural stability and electronic structure of InP NWs with first-principles quantum mechanics are strongly desirable to derive the microscopic properties of InP NWs.

In this study, we investigate structural stability and electronic properties of InP NWs vertically grown on InP(111) substrates from first-principles pseudopotential calculations with fully optimized geometry. Our calculations with diameter (D_{NW}) less than 23 Å demonstrate that the ZB NWs are less favorable over the WZ NWs, in which importantly the surface dangling bonds (DBs) on the NW facets are found to be crucial to determine the stability. An analysis of the NW cohesive energy based on the number of the DBs predicts that the NWs are bistable, forming both WZ and ZB structures at $D_{\mathrm{NW}} \approx 120$ Å, which leads to the exhibition of polytypes. In addition, our estimation of the optical properties in the WZ NWs demonstrates the blueshift of the transition energy and the enhancement of the oscillator strength, suggesting the possibility of efficient light emission in WZ NWs.

II. CALCULATION PROCEDURE

In order to discuss the structural stability during synthesis of InP NWs, we here employ pristine InP NWs as a representative of NW models. Since InP NWs are usually fabricated at relatively high temperature (~800 °C),[5,6,18,19] we assume that surface atoms on the NW facets during the synthesis are not saturated by foreign atoms such as H atoms. We consider the InP NWs in ZB and WZ structures with hexagonal shape which is assumed from crystal symmetry considerations. The ratio of the number of surface DBs generated on NW facets to the total number of atoms in each diameter is the lowest in the hexagonal shape, as shown in Fig. 1, leading to large NW cohesive energy for a certain diameter. The hexagonal ZB and WZ NWs are denoted as

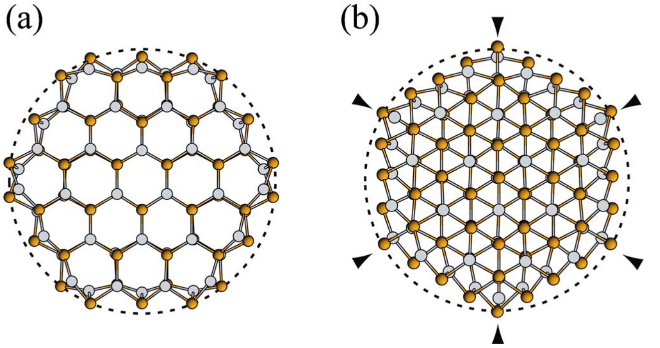

FIG. 1. (Color online) Cross-sectional view of hexagonal (a) WZ [WZ-H(54, 54)] and (b) ZB [ZB-H(42, 40, 40)] NWs. Gray (open) and brown (solid) circles represent In and P atoms, respectively. The D_{NW} of NW (dashed circle) is defined as the diameter of a circle precisely enclosing a hexagonal wire. Arrowheads indicate two-coordinated atoms located at the boundaries of NW facets.

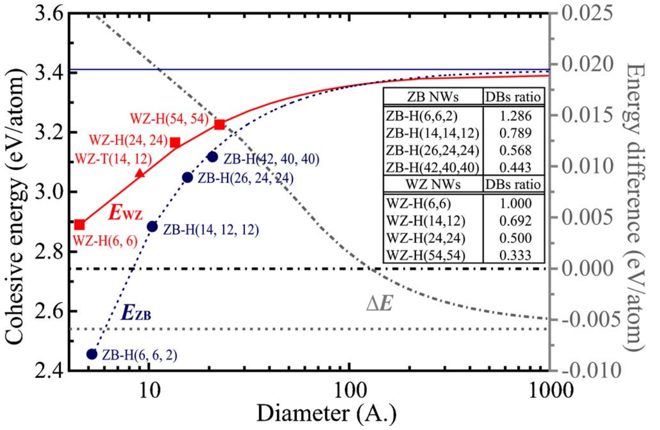

ZB NWs	DBs ratio
ZB-H(6,6,2)	1.286
ZB-H(14,14,12)	0.789
ZB-H(26,24,24)	0.568
ZB-H(42,40,40)	0.443
WZ NWs	**DBs ratio**
WZ-H(6,6)	1.000
WZ-H(14,12)	0.692
WZ-H(24,24)	0.500
WZ-H(54,54)	0.333

FIG. 2. (Color online) Cohesive energies of InP NWs as a function of nanowire diameter. Circles, squares, and triangles represent cohesive energies of ZB, hexagonal WZ, and triangle WZ NWs, respectively. Solid (red), dotted (blue), and dashed and dotted (gray) curves indicate the E_c of ZB NWs (E_{ZB}), that of hexagonal WZ NWs (E_{WZ}), and the energy difference ΔE between ZB and WZ NWs obtained from Eqs. (2) and (3), respectively. The horizontal solid (blue) line represents the bulk cohesive energy ($\varepsilon_0 = 3.41$ eV) and the dotted (gray) line the bulk energy difference between ZB and WZ structures ($\Delta\varepsilon = 5.6$ meV). The ratio of the number of surface DBs generated on the NW facets to the total number of atoms is also listed.

ZB-H(l, m, n) and WZ-H(l, m), respectively, where l, m, and n represent the number of atoms in each double layer. The WZ NW in a triangle shape, WZ-T(14, 13), is also considered in order to determine the relative stability between WZ and ZB structures at $D_{\mathrm{NW}} \approx 9.0$ Å.

The calculations are based on the generalized gradient approximation[30] (GGA) and norm-conserving pseudopotentials.[31] The conjugate-gradient technique[32,33] is utilized both for the electronic structure calculation and for the geometry optimization. We employ a supercell in which a nanowire is placed with its facets being separated by ~7 Å from those of adjacent NWs. We adopt the partial core correction for In atoms in the treatment of the exchange-correlation energy.[34] The valence wave functions are expanded by the plane-wave basis set with a cutoff energy of 20.25 Ry which gives an enough convergence of total energy to discuss the relative stability: The cohesive energy of ZB InP in the bulk (3.41 eV) and the energy difference between WZ and ZB structures (5.6 meV/atom) agree well with previous calculations.[35] The k-point sampling for integration over the one-dimensional Brillouin zone (BZ) is carefully chosen to maximize the accuracy: The four k points for cubic structure and the six k points for hexagonal structure, both of which are folded into the two k-point sampling in the least common multiplied supercell with six double layers, are found to provide sufficient accuracy in the total energies.

III. RESULTS AND DISCUSSION

A. Structural stability

The stability of NWs is discussed in terms of the cohesive energy E_c defined as

$$E_c = \left\{ \sum_{\beta} n_\beta \mu_\beta - E_{tot} \right\} \Big/ \sum_{\beta} n_\beta, \tag{1}$$

where E_{tot} is the total energy of the supercell containing an InP NW, μ_β is the chemical potential of β atoms (β=In, P) in the supercell, and n_β is the number of β atoms. The chemical potentials of In and P atoms are chosen as the values of μ_{In} and μ_{P}, respectively. Figure 2 shows the E_c of InP NWs with $D_{\mathrm{NW}} \leq 23$ Å by using Eq. (1). As the D_{NW} increases, E_c converges into the calculated bulk cohesive energy. The behavior of E_c with respect to D_{NW} correspondsto the decrease of the surface DB ratio. In contrast to the bulk phase, importantly, the ZB NWs are less energetically favorable than the WZ NWs whose diameter is close to that of the ZB NWs, over the entire range of D_{NW} considered here. This is because the structural stability is mainly determined by the surface DBs on the NW facets. On the facets of both WZ [Fig. 1(a)] and ZB [Fig. 1(b)] NWs, there are three-coordinated In and P atoms bonded with each other. Instead, In-P pairs, each of which consists of two- and three-coordinated atoms, are inevitably formed in the surface boundaries of the ZB NW facets, as indicated by arrowheads in Fig. 1(b). The presence of two-coordinated atoms leads to a higher surface DB ratio in the ZB NWs compared with that in the WZ NWs with close D_{NW}, as listed in Fig. 2. Since dangling bonds in semiconductors generally induce a large energy loss in the cohesive energy, the high DB ratio in ZB NWs results in destabilization of the ZB structure.

Our analysis of the E_c by considering the energy contribution of the surface DBs and the energy difference between WZ and ZB structures in the bulk phase $\Delta\varepsilon$ shows that a simple description of E_c can reproduce these structural characteristics. We express the cohesive energies of the WZ NW E_{WZ} and of the ZB NW E_{ZB} as

$$E_{\mathrm{WZ}} = \varepsilon_0 - \Delta\varepsilon - \frac{N_{\mathrm{DB}}^{(1)}}{N_{tot}} E_{\mathrm{DB}}^{(1)}, \tag{2}$$

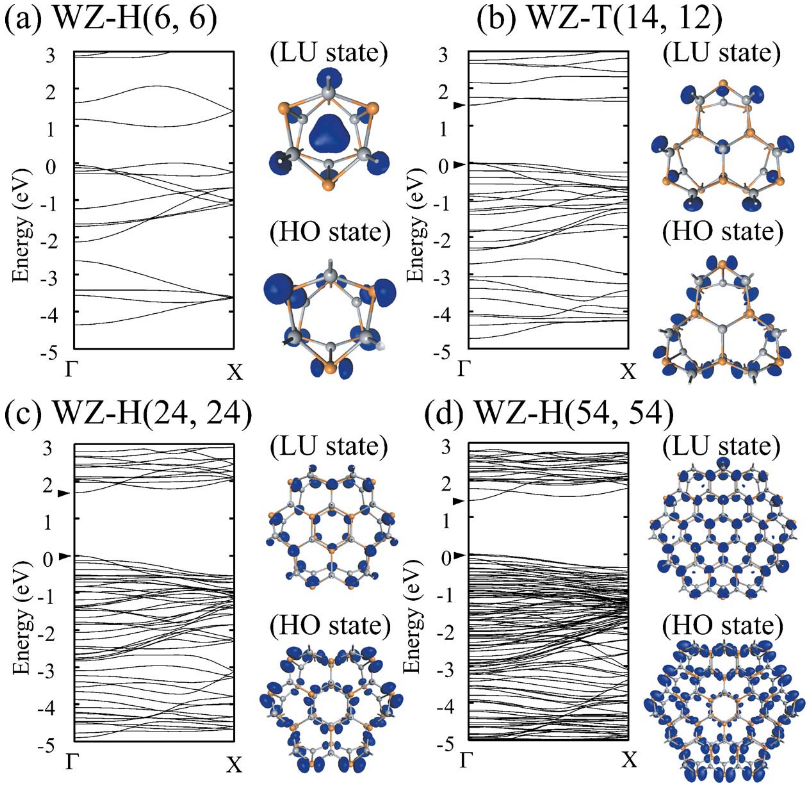

FIG. 3. (Color online) Energy bands (Kohn-Sham energy levels) and cross-sectional views of NWs with isosurface of the wave function for the highest occupied (HO) and lowest unoccupied (LU) states in (a) WZ-H(6, 6), (b) WZ-T(14, 12), (c) WZ-H(24, 24), and (d) WZ-H(54, 54). Energies are measured from the HO band. Arrowheads in energy bands indicate the electronic states involved in the largest dipole matrix element responsible for the oscillator strength shown in Table I.

$$E_{\mathrm{ZB}} = \varepsilon_0 - \frac{N_{\mathrm{DB}}^{(1)}}{N_{tot}} E_{\mathrm{DB}}^{(1)} - \frac{N_{\mathrm{DB}}^{(2)}}{N_{tot}} E_{\mathrm{DB}}^{(2)}, \qquad (3)$$

respectively. Here, ε_0 is the bulk cohesive energy with ZB structure, N_{tot} the total number of atoms in the unit cell, $N_{\mathrm{DB}}^{(1)}$ ($N_{\mathrm{DB}}^{(2)}$) the total number of DBs for three- (two-) coordinated atoms in the unit cell, and $E_{\mathrm{DB}}^{(1)}$ ($E_{\mathrm{DB}}^{(2)}$) the energy loss due to surface DBs of three- (two-) coordinated atoms. Figure 2 also depicts E_{W} and E_{ZB} as a function of D_{NW}. The values of $E_{\mathrm{DB}}^{(1)}=0.50$ eV and $E_{\mathrm{DB}}^{(2)}=0.47$ eV are found to reproduce the calculated E_c, indicating applicability of the simple description of cohesive energy using Eqs. (2) and (3) to the stability of InP NWs with large D_{NW}.

For large D_{NW}, the energy contribution of surface DBs becomes negligible and the bulk energy difference $\Delta\varepsilon$ caused by the electrostatic interactions of ions and valence electrons[36] is dominant. As shown in Fig. 2, the energy difference between WZ and ZB structures, $\Delta E(=E_{\mathrm{WZ}}-E_{\mathrm{ZB}})$, using Eqs. (2) and (3) slowly converges into $-\Delta\varepsilon$ as D_{NW} increases. Since the most stable crystal structure of InP in the bulk form is the ZB structure, this trend with respect to D_{NW} shows the appearance of the bulk nature in large D_{NW}. Importantly, InP NWs possess the critical diameter at $D_{\mathrm{NW}} \approx 120$ Å, where they are bistable, forming both WZ and ZB structures. This implies that InP NWs around 120 Å diameter often exhibit polytypes.[40] Furthermore, ΔE for $D_{NW} \geq 120$ Å($\sim$0.003 eV/atom) is found to be lower than that in the bulk phase. Since the small energy difference between WZ and ZB structures often induces twin structures as reported in bulk ZnSe,[37] the small energy difference between WZ and ZB structures in InP NWs suggests that the WZ segments could be incorporated in the ZB NWs even around 400 Å diameter. Although further elaborate investigations for the formation of rotational twin structures at finite temperature might be necessary in order to interpret the experimental results quantitatively, the present result is qualitatively consistent with the TEM observation of rotational twin structures.[18]

B. Electronic structure

Figure 3 shows the calculated (Kohn-Sham) energy bands near the HO state of stable WZ NWs, such as WZ-H(6, 6), WZ-T(14, 12), WZ-H(24, 24), and WZ-H(54, 54). As shown in Fig. 3, the effects of the surface DBs on the NW facets as well as the NW size on the electronic structure can be seen in the WZ NWs.[38] For InP NWs with $D_{\mathrm{NW}} \leq 9$ Å, such as WZ-H(6, 6) and WZ-T(14, 12), the surface DB states determine the band character and gap energy, whereas the gap energy of NWs with $D_{\mathrm{NW}} \geq 13.5$ Å, such as WZ-H(24, 25) and WZ-H(54, 54), is dependent on only the NW size, as explained below. Although the GGA calculation might be limited in clarifying the electronic structure of InP NWs accurately,[39] characteristics in the electronic structure could be qualitatively evaluated from the present results.

The spatial distributions of the wave functions for the HO and the LU states in WZ-H(6, 6) [Fig. 3(a)] and WZ-T(14, 12) [Fig. 3(b)] exhibit a localized character around three-coordinated atoms. This localized nature indicates that the HO (LU) state corresponds to the DB states of P (In) atoms in three-coordinated In-P pairs. Furthermore, it is found that the peaks of the local density of states (LDOS) for surface In (P) atom of these NWs [Figs. 4(a) and 4(b)] appear in the LU

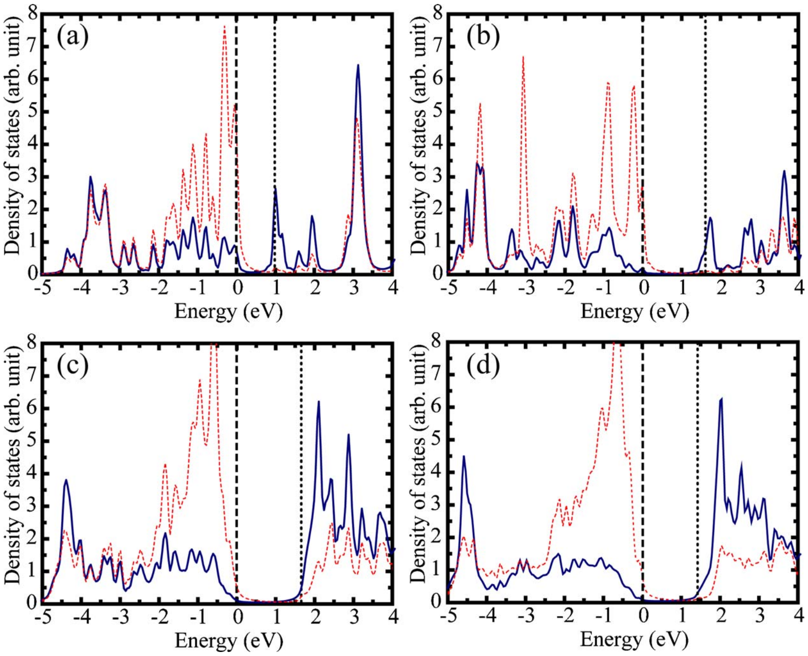

FIG. 4. (Color online) Local density of states (LDOS) of surface atoms for (a) WZ-H(6, 6), (b) WZ-T(14, 12), (c) WZ-H(24, 24), and (d) WZ-H(54, 54). Solid (blue) and dashed (red) lines represent LDOS of In and P atoms, respectively. Vertical dashed and dotted lines indicated the HO and LU states, respectively. Energies are measured from the HO band.

(HO) state. These results clearly show that the HO and LU states corresponds to the DB states of P and In atoms in three-coordinated In-P pairs, respectively. In WZ-H(6,6) the short distances between neighboring In-P pairs (~2.58 Å) induce the hybridization of the DB states and cause the band dispersion of 0.2 (0.7) eV in the HO (LU) band. Due to the large dispersion for the LU band, WZ-H(6,6) possesses an indirect semiconducting character. On the other hand, the distances between neighboring In-P pairs in WZ-T(14, 12) (~3.37 Å) lead to relatively small dispersions (~0.2 eV) in the HU and LU bands. This leads to a direct allowed energy gap of 1.58 eV at the zone center in WZ-T(14, 12).

In WZ-H(24, 24) and WZ-H(54, 54), the localized DB states originating from the surface DBs of three-coordinated P atoms are resonant with valence bands and those of three-coordinated In atoms are located above the LU states. The wave function of the HO (LU) state in these NWs [Figs. 3(c) and 3(d)] corresponds to the bulk valence (conduction) band. The LDOS for surface In (P) atom of these NWs [Figs. 4(c) and 4(d)] clearly shows a semiconducting nature: The electronic states associated with DBs are located away from the band-gap region. These features thus indicate that the optical allowed gap appears at the zone center. Moreover, we find that the gap energy (1.45–1.69 eV) is found to be larger than that of the bulk InP (1.0 eV) and decreases as the $D_{\rm NW}$ increases. Since our analysis of the density of states (not shown here) finds that the conduction band with bulklike nature is located 3.0 and 2.1 eV above the bulklike valence band for WZ-H(6, 6) and WZ-T(14, 12), respectively, the size dependence of the gap energy can be interpreted as a quantum size effect, as seen in Si NWs.[24–27]

The direct band-gap characteristic in WZ-T(14, 12), WZ-H(24, 24), and WZ-H(54, 54) implies the possibility of efficient light emission. We thus estimate the "relative" oscillator strength $f_{\rm NW}/f_{\rm bulk}$ of InP NWs ($f_{\rm NW}$ and $f_{\rm bulk}$ are the oscillator strength of nanowire and that of bulk InP, respectively) expressed as

$$\frac{f_{\rm NW}}{f_{\rm bulk}} = \frac{\omega_{\rm bulk}}{\omega_{\rm NW}}\left|\frac{d_{\rm NW}}{d_{\rm bulk}}\right|^2 \frac{\pi\rho_{\rm NW}(a_{\rm B}^{\rm bulk})^3|G(\zeta=0)|^2}{\sigma_{\rm NW}}, \qquad (4)$$

where $\omega_{\rm NW}$ ($d_{\rm NW}$) is the transition energy (dipole matrix element), $\sigma_{\rm NW}$ the cross section, $\rho_{\rm NW}$ the volume filing factor, and $G(\zeta)$ with ζ being the relative coordinate of an electron and a hole an exciton envelope function.[24,25] Since the present GGA calculation for bulk InP underestimates the gap energy by ~68%,[39] we here correct the calculated conduction-band levels of the WZ NWs by using the scissors operator which makes the calculated gap energy of the bulk InP coincide with the experimental value (1.42 eV). The $\omega_{\rm bulk}$ ($d_{\rm bulk}$) is the transition energy (transition matrix elements) and $a_{\rm B}^{\rm bulk}$ is the effective Bohr radius of the exciton in the bulk InP. We note that only the lowest-energy bound state with singlet spin configuration is of interest. Considering the PL measurement performed at room temperature, we estimate the $f_{\rm NW}/f_{\rm bulk}$ among the transition from the HO band and the states below the HO band within 0.03 eV to the LU band and the states above the LU band within 0.03 eV. Table I shows the $f_{\rm NW}/f_{\rm bulk}$ among these transitions, together with $D_{\rm NW}$, the effective Bohr radius $a_{\rm B}^{\rm NW}$, and the exciton binding energy E_{bind}. The $a_{\rm B}^{\rm NW}$ (26–30 Å) with large oscillator strength (the electronic states are indicated by arrowheads in Fig. 3) shows that the excitons have a large spatial extent in comparison with the diameters, resulting in two-dimensional squeezing of their wave function. We see that the E_{bind} increases as the $D_{\rm NW}$ decreases. The size dependence of E_{bind} qualitatively agrees with the previous results for Si NWs.[24–26] Moreover, one-dimensional exciton effects are found to enhance the oscillator strength. These results thus indicate that the geometrical restriction of the excitons dramatically enhances the oscillator strength of the optical transition, suggesting the possibility of efficient light emission from InP NWs with small $D_{\rm NW}$. Since the transition for the largest oscillator strength in the WZ-T(14, 12) corresponds to

TABLE I. Relative oscillator strength $f_{\mathrm{wire}}/f_{\mathrm{bulk}}$ among the transitions from the HO band and the states below the HO band within 0.03 eV to the LU state of the WZ-T(14, 12), WZ-H(24, 24), and WZ-H(54, 54). The diameter D_{NW}(Å), effective Bohr radius a_{NW}(Å), exciton binding energy E_{bind} (eV), and energy gap corrected by the scissor operator E_g' (eV) are also shown.

Nanowire	D_{NW}	Transition	a_{NW}	E_{bind} (E_g')	$f_{\mathrm{NW}}/f_{\mathrm{bulk}}$
WZ-T(14,12)	9.0	HO-2/LU	16.9	0.42 (2.04)	0.30
		HO-1/LU	29.8	0.51 (2.03)	59.7
		HO/LU	17.7	0.40 (2.03)	0.01
WZ-H(24,24)	13.5	HO/LU	28.1	0.17 (2.13)	27.4
WZ-H(54,54)	22.5	HO-1/LU	27.2	0.03 (1.92)	12.6
		HO/LU	27.9	0.04 (1.89)	0.00

the transition between the HO and LU states, the localized DB states crucially affect the optical property. However, such a large oscillator strength is unable to be obtained in the PL measurement because the DB states should be eliminated by the covered oxide layer which is believed to be formed after removal of the NWs from the growth apparatus.[6] In contrast, the electronic states responsible for the optical transition in WZ-T(24, 24) and WZ-T(54, 54) are delocalized and possess bulklike nature. Therefore, it is likely that a large oscillator strength and significant blueshift in the PL data are obtained even in passivated WZ-H(24, 24) and WZ-T(54, 54). Although the present results cannot be directly compared with the PL data[6,18] because the diameters considered in this study are much smaller than those of abundant InP NWs in experiments, trends in the optical properties in WZ-T(24, 24) and WZ-T(54, 54) are qualitatively consistent with experimental results.

IV. SUMMARY

We have found that the InP NWs with WZ structure are stabilized for small diameter due to a contribution of surface dangling bonds on the NW facets to the cohesive energy. The bistability of InP NWs forming both WZ and ZB structures at large diameter around 120 Å implies exhibition polytypes. We have also found that the stable WZ NWs are semiconducting whose characteristics are dependent on the NW size and shape. The estimated oscillator strength for the WZ NWs indicates the possibility of efficient light emission from InP NWs originating from direct-gap and geometrically restricted excitonic effects.

Note added. Very recently, InP nanowires with wurtzite structure were fabricated by selective-area growth.[41]

ACKNOWLEDGMENTS

One of us (T.A.) would like to thank H. Kageshima and A. Taguchi for their discussions and comments. Codes used in this work are based on the Tokyo *ab-initio* program package (TAPP). Computations were partly done at RCCS (National Institutes of Natural Sciences) and ISSP (University of Tokyo).

---

*Electronic address: akiyama@phen.mie-u.ac.jp

[1] R. S. Wagner and W. C. Elis, Appl. Phys. Lett. **4**, 89 (1964).
[2] R. F. Seervice, Science **294**, 2442 (2001).
[3] A. M. Morales and C. M. Lieber, Science **279**, 208 (1998).
[4] X. Duan and C. M. Lieber, Adv. Mater. (Weinheim, Ger.) **12**, 298 (2000).
[5] X. Duan, Y. Huang, Y. Cui, J. Wang, and C. M. Lieber, Nature (London) **409**, 66 (2001).
[6] M. S. Gudiksen, J. Wang, and C. M. Lieber, J. Phys. Chem. B **105**, 4062 (2001).
[7] J. Wang, M. S. Gudiksen, X. Duan, Y. Cui, and C. M. Lieber, Science **293**, 1455 (2001).
[8] M. S. Gudiksen, L. J. Lauhon, J. Wang, D. C. Smith, and C. M. Lieber, Nature (London) **415**, 617 (2002).
[9] N. Ozaki, Y. Ohno, and S. Takeda, Appl. Phys. Lett. **73**, 3700 (1998).
[10] Ji. Liu, X.-M. Meng, Y. Jiang, C.-S. Lee, I. Bello, and S.-T. Lee, Appl. Phys. Lett. **83**, 4241 (2003).
[11] J. Kikkawa, Y. Ohno, and S. Takeda, Appl. Phys. Lett. **86**, 123109 (2005).
[12] L. J. Lauhon, M. S. Gudiksen, D. Wang, and C. M. Lieber, Nature (London) **420**, 57 (2002).
[13] X. Duan, C. Niu, V. Sahi, J. Chen, J. W. Parce, S. Empedocles, and J. L. Goldman, Nature (London) **425**, 274 (2003).
[14] Y. Wu, Y. Cui, L. Huynh, C. J. Barrelet, D. C. Bell, and C. M. Lieber, Nano Lett. **4**, 433 (2004).
[15] M. Yazawa, M. Koguchi, and K. Hiruma, Appl. Phys. Lett. **58**, 1080 (1991).
[16] M. Koguchi, H. Kakibayashi, M. Yazawa, K. Hiruma, and Toshio Katsuyama, Jpn. J. Appl. Phys., Part 1, **31**, 2061 (1992).
[17] K. Hiruma, M. Yazawa, T. Katsuyama, K. Ogawa, K. Haraguchi, M. Koguchi, and H. Kobayashi, J. Appl. Phys. **77**, 447 (1995).
[18] S. Bhunia, T. Kawamura, Y. Watanabe, S. Fujikawa, and K. Tokushima, Appl. Phys. Lett. **83**, 3371 (2003).
[19] M. Akabori, J. Tanaka, J. Motohisa, and T. Fukui, Nanotechnology **14**, 1071 (2003).
[20] J. D. Holmes, K. P. Johnston, R. C. Doty, and B. A. Korgel, Science **287**, 1471 (2000).
[21] Y. F. Chan, X. F. Duan, S. K. Chan, I. K. Sou, X. X. Zhang, and N. Wang, Appl. Phys. Lett. **83**, 2665 (2003).
[22] X. Duan, Y. Huang, R. Agaewal, and C. M. Lieber, Nature (London) **421**, 241 (2003).
[23] D. D. D. Ma, C. S. Lee, F. C. K. Au, S. Y. Tong, and S. T. Lee, Science **299**, 1874 (2003).
[24] T. Ohno, K. Shiraishi, and T. Ogawa, Phys. Rev. Lett. **69**, 2400 (1992).
[25] G. D. Sanders and Y. C. Chang, Phys. Rev. B **45**, 9202 (1992).
[26] C. -Y. Yeh, S. B. Zhang, and A. Zunger, Phys. Rev. B **50**, 14405 (1994).
[27] X. Zhao, C. M. Wei, L. Yang, and M. Y. Chou, Phys. Rev. Lett.

92, 236805 (2004).

[28] R. Rurali and N. Lorente, Phys. Rev. Lett. **94**, 026805 (2005).

[29] T. Y. Tan, N. Li, and U. Gösele, Appl. Phys. Lett. **83**, 1199 (2003).

[30] J. P. Perdew, K. Burke, and M. Ernzerhof, Phys. Rev. Lett. **77**, 3865 (1996).

[31] N. Troullier and J. L. Martins, Phys. Rev. B **43**, 1993 (1991).

[32] J. Yamauchi, M. Tsukada, S. Watanabe, and O. Sugino, Phys. Rev. B **54**, 5586 (1996).

[33] H. Kageshima and K. Shiraishi, Phys. Rev. B **56**, 14985 (1997).

[34] S. G. Louie, S. Froyen, and M. L. Cohen, Phys. Rev. B **26**, 1738 (1982).

[35] C. -Y. Yeh, Z. W. Lu, S. Froyen, and A. Zunger, Phys. Rev. B **45**, R12130 (1992).

[36] T. Ito, Jpn. J. Appl. Phys., Part 2, **37**, L1217 (1998).

[37] A. G. Fisher, J. Electrochem. Soc. **106**, 830 (1959).

[38] The energy band characters of the ZB NWs are quite different from those of the WZ NWs. The distances between two-coordinated In and P atoms (~7.9 Å) preclude electron transfer between two-coordinated counterparts, resulting in the appearance of partially occupied localized states in the energy gap.

[39] We actually find that the calculated gap energy of the bulk InP (1.0 eV) underestimates the observed one (1.42 eV).

[40] The estimated value of diameter, due to the slightly crude treatment for the cohesive energy, might include a few nanometer of errors. We actually find that the error of 0.01 eV in the energy of DBs induces the errors of 10 Å in the critical diameter. However, the structural trends could be qualitatively reproduced by the present description.

[41] P. Mohan, J. Motohisa, and T. Fukui, Nanotechnology **16**, 2903 (2005).